

**SZENT ISTVÁN UNIVERSITY**

**DEVELOPMENT OF NOVEL CRYOPRESERVATION  
METHOD FOR MAMMALIAN OOCYTE**

**Jun Liu**

GÖDÖLLŐ

2009

## The PhD program

**Name:** Animal Husbandry Science PhD School

**Discipline:** Animal Husbandry Science

**Leader:** **Prof. Dr. Miklós Mézes DSc**  
Head of Department,  
Szent István University, Faculty of Agricultural and Environmental Sciences,  
Department of Nutrition

**Supervisor:** **Prof. Dr. András Dinnyés, DSc**  
Head of Molecular Animal Biotechnology Laboratory,  
Szent István University, Faculty of Agricultural and Environmental Sciences,  
Institute for Basic Animal Sciences

.....  
Approval of the PhD School Leader

.....  
Approval of the Supervisor

# 1 INTRODUCTION

Mammalian oocyte cryopreservation has applications in animal agriculture, biomedical research, human reproductive medicine and biodiversity preservation. Currently, most oocyte cryopreservation protocols have been direct, or slight modifications of the methods developed for embryos. These were primarily developed by trial and error adjustments of cooling and warming rates, and choice of CPA and CPA concentration. However, because there are a large number of protocol variables potentially affecting cell viability, an exhaustive experimental search for the optimal combination of these parameters would be prohibitively expensive in terms of time and resources. Recently, it has been realized that a fundamental understanding of the nature of damage to oocytes during the multiple steps involved in the cryopreservation procedure, such as CPA addition/removal, cooling, and intracellular ice formation temperature, is crucial. The ability for successful cryopreservation of mammalian oocytes is highly dependant upon an understanding of the fundamental cryobiological factors that determine viability or death post-thaw.

Cryopreservation methods can be developed by theoretically examining biophysical events during the processes of the cryopreservation. These events include the movement of intracellular water and permeating cryoprotectant across the plasma membrane prior to, during and after freezing, ice formation, vitrification and thawing. During a cryopreservation procedure, cellular status such as cell water volume and intracellular solute concentration can be calculated by established equations along with corresponding parameters. The kinetics of these statuses are dependent on the intrinsic cellular characteristics, such as membrane permeability coefficients and related activation energies, and external conditions applied, such as equilibrated CPA concentrations, cooling rates and warming rates, and they are intimate related to the probability of intracellular ice formation (cell damage). This thesis presents the methodology of utilizing theoretical models for the development of cryopreservation protocols by designing specific cooling profiles and selecting appropriate external conditions to optimize the cryopreservation survivals.

This thesis includes essential materials from several stand-alone peer-reviewed publications. In Chapter 2, all essential equations that govern biophysical events during a cryopreservation procedure are presented. Chapter 3 presents the published method of theoretically optimizing an ISF protocol. Chapter 4 presents the published accumulative osmotic damage model (AOD) for oocyte cryopreservation. In Chapter 5, the research on the development of a novel cryopreservation three-step method for mammalian oocyte is presented.

## 2 THEORY OF FUNDAMENTAL CRYOBIOLOGY

### 2.1 Mathematical formulation of the membrane permeability coefficients

Two coupled equations depicting the changes of intracellular water volume and the mole number of CPA during temperature changes with cooling rate of  $B$  in the presence of extracellular ice were derived for the first time:

$$\frac{dV_w}{dT} = -\frac{ARTL_p(T)}{v_{10}B} \left[ \ln\left(\frac{V_w}{V_w + (n_n^i + n_s^i)v_{10}}\right) + \ln\left(1 + \frac{G'C(T)}{100 - C(T)}\right) \right] \quad (2.1)$$

$$\frac{dn_s^i}{dT} = \frac{AP_s(T)}{B} \left( \frac{1000R_t C}{MW_s(100 - C)(R_t + 1)} - \frac{n_s^i}{V_w} \right). \quad (2.2)$$

These equations represent a theoretical model incorporating the trans-membrane movement of cryoprotectant during cryopreservation procedures. This model is used to investigate the responses of cells to cryopreservation procedures by simulating the kinetics of cell water volume, intra- and extracellular solute concentrations, the degree of supercooling of the cytoplasm, and the probability of intracellular ice nucleation.

### 2.2 Activation energies and phase diagram

The Arrhenius relationship is used to describe the temperature dependence of permeability parameters  $L_p$  and  $P_s$ . The value of any parameter  $P_a$  ( $L_p$  or  $P_s$ ) at any temperature  $T$  can be obtained by the following formula:

$$P_a(T) = P_{ao} \cdot \exp\left[\frac{E_a}{R} \left(\frac{1}{T_o} - \frac{1}{T}\right)\right]. \quad (2.3)$$

Ternary phase diagram is used to calculate extracellular solute concentrations.

$$T_m = A_1C + B_1C^2 + C_1C^3 \quad (2.4)$$

### 2.3 Calculation of the probability of intracellular ice formation ( $P_{\text{IIF}}$ )

The probability of intracellular ice formation is calculated by considering the three mechanisms of homogeneous nucleation (HOM), surface-catalyzed nucleation (SCN), and volume-catalyzed nucleation (VCN):

$$P_{\text{IIF}} = 1 - \left(1 - P_{\text{IIF}}^{\text{HOM}}\right) \cdot \left(1 - P_{\text{IIF}}^{\text{SCN}}\right) \cdot \left(1 - P_{\text{IIF}}^{\text{VCN}}\right) \quad (2.5)$$

$$PIIF^j = 1 - \exp \left\{ \int_{t_o}^{t_f} \Omega_j \exp \left[ - \frac{\kappa_j \cdot T_m^5}{(T_m - T)^2 \cdot T^3} \right] \cdot V \cdot dt \right\} \quad (2.6) \quad \text{where } j$$

= HOM, SCN and VCN.

These integration limits ( $t_o$  and  $t_f$ ) are referred to the starting and ending points of the period, during which the  $P_{IIF}$  is calculated. The values of the parameters required for these calculations can be determined by fitting equations to the experimental data of  $P_{IIF}$ .

### 3 A THEORETICAL MODEL FOR THE DEVELOPMENT OF INTERRUPTED SLOW FREEZING PROCEDURES

The objective of the present study was to theoretically optimize an ISF protocol to cryopreserve rat zygotes. Essentially, development of the model followed three steps: (1) an initial range of DMSO concentrations from 0 to 4 Molal, and a range of cooling rates from 0 to 2.5°C/min were evaluated theoretically to determine the selections of  $[CPA]^0$  and  $B_1$  that would allow the  $[S]^i$  to reach the  $[CPA]_c$ ; (2) using Mazur's IIF model, the selections that could result in IIF were eliminated; and (3) the associated plunging temperatures for the combinations of  $[CPA]^0$  and  $B_1$  ranges were then calculated. The optimum set of conditions from the final range was then selected based on minimum duration of slow cooling.

#### 3.1 Materials and methods

##### *Theoretical Prediction of Intracellular Water Volume and Solute Mole Number at Varying Temperatures*

During slow cooling, temperature is typically decreased linearly causing the intracellular solute concentration to increase monotonically. For a specific cell and CPA, the change in the intracellular CPA concentration is affected by cooling conditions, i.e. the  $B_1$  of the process and the  $[CPA]^0$  loaded into cells prior to the onset of freezing. Using above equations, it is possible to quantitatively calculate: (i) the change in cell water volume vs. temperature during cooling; (ii) the change in  $[S]^i$  vs. temperature; and (iii) the change in extracellular solute concentration vs. temperature.

##### *Assumptions Pertaining to Intracellular Ice Formation (IIF)*

The present method makes assumptions based upon Mazur's "three requirements" for IIF: (1) the sample temperature has reached the ice nucleation zone, or in other words, the temperature has become lower than the nucleation temperature; (2) the intracellular water content at that time is  $\geq 10\%$  of its isotonic value; and (3) the intracellular water is 2°C or more supercooled. Based upon these criteria, IIF will not occur if any one of these requirements is not met.

##### *Prediction of the Theoretically Optimized Cryopreservation Protocol*

The procedure for theoretical optimization involved three steps. First, the  $[CPA]_c$  was determined based on measurement of  $B_2$  and  $B_3$  inside the straws. Next, the initial investigation ranges for  $[CPA]^0$  and

$B_1$  were determined and these ranges were quantized into appropriate intervals for subsequent numerical calculation of  $[S]^i$  and degree of supercooling. In the final step of model development, combinations of  $[CPA]^0$  and  $B_1$  values that could be used were determined and the  $T_p$  values for these combinations were calculated. The optimum set of conditions can then be selected by the minimum duration of slow cooling, which minimizes solution effects. In this study,  $[CPA]^0$  values ranging from 0 to 4 molal were chosen in conjunction with  $B_1$  values ranging from 0 to  $-2.5^\circ\text{C}/\text{min}$ . These ranges were then divided into fifty equal intervals. For each of these 2500 (50X50) combinations of  $[CPA]^0$  and  $B_1$ , the intracellular CPA concentration, intracellular water volume and extent of supercooling at each temperature point were calculated. The intracellular concentration for each combination of  $[CPA]^0$  and  $B_1$  was calculated at each temperature point starting from  $T_{\text{seed}}$  to  $T_{\text{end}}$ , and the value was compared to the  $[CPA]_c$ . The extent of supercooling and intracellular water volume was then calculated for the temperature points that fell below the nucleation temperature to determine if IIF would occur based on Mazur's "three requirements". Any combination that would likely result in IIF was then ruled out. If the  $[S]^i$  could not reach the  $[CPA]_c$  over the entire temperature range, this combination of  $[CPA]^0$  values and  $B_1$  values were also ruled out. The remaining points were considered the optimum range for plunging in  $\text{LN}_2$  for that particular combination of  $[CPA]^0$  and  $B_1$  values.

## 3.2 Results

### *Calculations of Optimal Plunging Temperature*

The criteria of  $[CPA]_c$  exceeding 40% (w/w) and no predicted IIF were used to divide the plane of  $[CPA]^0$  vs.  $B_1$  into three regions (Figure 3.1) as follows:

Region I: in this region, no combination of  $[CPA]^0$  and  $B_1$  allows the intracellular solute concentration to reach the  $[CPA]_c$  at any temperature point. This region contains the high cooling rate zone and low initial CPA concentration zone.

Region II: The combinations of  $[CPA]^0$  and  $B_1$  allow the  $[S]^i$  to reach  $[CPA]_c$  at certain temperature points, but under these conditions there is a high probability of IIF during slow cooling. These conditions were also rejected in developing the ISF procedure.

Region III: The combinations of  $[CPA]^0$  and  $B_1$  allow the  $[S]^i$  to reach the  $[CPA]_c$ , and no IIF is predicted during slow cooling.

Figure 3.2 shows the  $T_p$  for each  $[CPA]^0$  and  $B_1$ , indicated by the 2-dimensional plot. The optimum protocol has been determined to be: a  $[CPA]^0$  of 1.2 M DMSO, a  $B_1$  of  $0.95^\circ\text{C}/\text{min}$  and  $T_p$  of  $-35^\circ\text{C}$ , based on minimum duration of slow cooling.

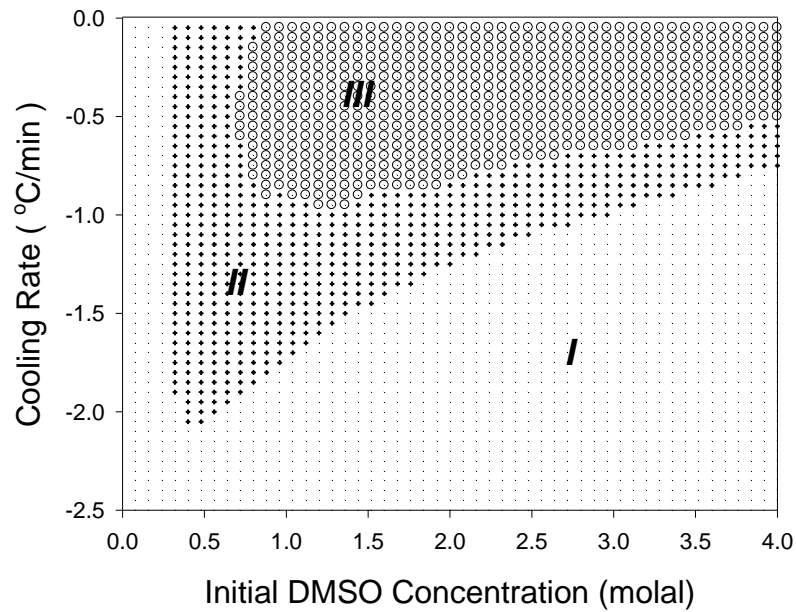


Figure 3.1. A diagram showing the plane of initial CPA concentration and cooling rate is divided into three regions.

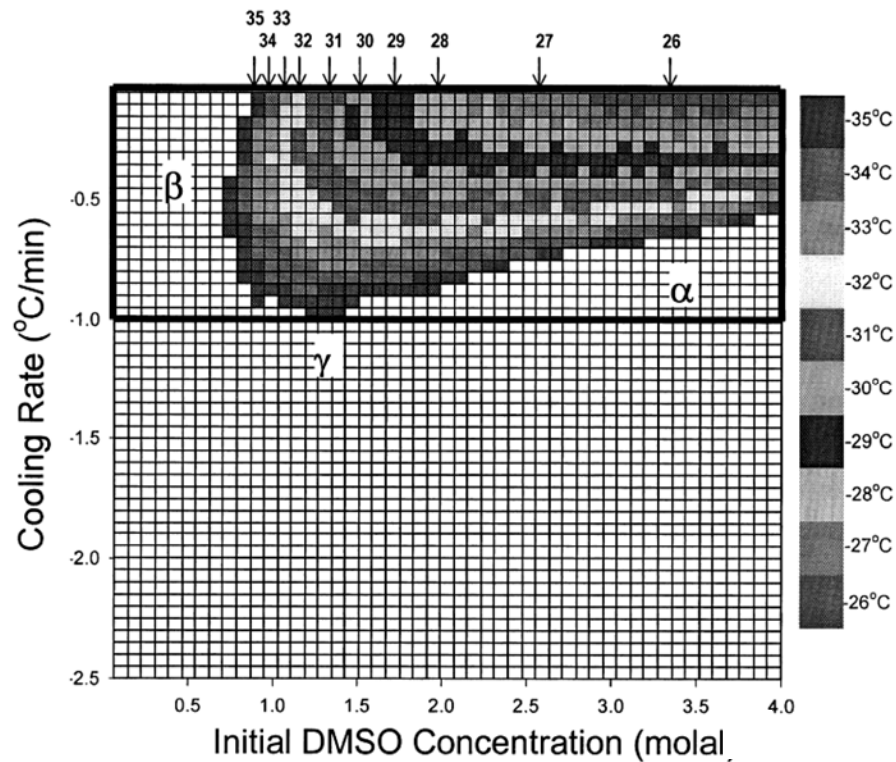


Figure 3.2. Plunging temperatures for each combination of initial CPA concentration ( $[CPA]^0$ ) and cooling rate ( $B_1$ ) in Region III of Figure 3.1. The gray level coded plot of plunging temperatures shows the exact values (indicated in  $^{\circ}C$ ).

### 3.3 Discussion

In contrast to previous publications, in the model described here, the changes of intracellular water volume and  $[S]^i$  during cooling and warming were predicted considering that the cell remains permeable to CPA at low temperatures. Mazur's model agreed closely with experimental data and was therefore

considered adequate. In Karlsson *et al.*'s study, a cost function was used to optimize the duration time of the freezing protocol, and this has been accomplished in a simplified manner in the current model by calculating the duration of slow cooling. For the rat zygote, this optimal  $[\text{CPA}]^0$  changes slightly for different  $B_1$  values. When the  $B_1$  increases from  $0.1^\circ\text{C}/\text{min}$  to  $0.95^\circ\text{C}/\text{min}$ , the optimal  $[\text{CPA}]^0$  decreases from 1.7 Molal to 1.2 Molal. However, these optimal conditions occur right on the border of regions where unacceptable cell damage is predicted. Therefore, though theoretically optimal, this set of conditions may actually be risky in practice, because any procedural error (e.g., fluctuation in cooling rate, error in solution preparation) or error in solution properties (e.g., error in  $[\text{CPA}]_c$  estimation) could result in unexpected negative consequences. Indeed, the determination of Zone III is very sensitive to the value of  $[\text{CPA}]_c$ . By selecting a point more towards the center of Zone III, (e.g. a  $[\text{CPA}]^0$  of 1.5 Molal DMSO, a  $B_1$  of  $0.5^\circ\text{C}/\text{min}$  and a  $T_p$  of  $-30^\circ\text{C}$ ) a more conservative estimation can be achieved.

The current research results suggest an alternative way to cryopreserve mammalian embryos and oocytes. The  $[\text{CPA}]_c$  is constrained by the  $B_2$  during plunging and  $B_3$  during thawing for a given solution. It is important to note that if these rates could be increased by using a thinner container, or material with higher heat transfer properties, then  $[\text{CPA}]_c$  may be reduced. This would result in situations where controlled cooling could be performed much more efficiently by applying higher  $B_1$  values and lower  $[\text{CPA}]^0$  values. These conditions would appear to be optimal because the higher  $B_1$  shortens the duration of slow cooling (therefore potentially reducing solution effects injury), and the lower  $[\text{CPA}]^0$  lowers the osmotic stress and lessens the potential CPA toxicity.

## **4 ACCUMULATIVE OSMOTIC DAMAGE MODEL FOR OOCYTE CRYOPRESERVATION**

The objective of the current study was to experimentally determine osmotic characteristics of rabbit oocytes. Using computer modeling, the rabbit oocyte volume responses during the cryoprotectant agent (CPA) addition and dilution procedures were investigated, and these responses were compared to the developmental ability of the oocytes to blastocysts in culture. The results of this comparison led to the establishment of a new model to describe the accumulative osmotic damage (AOD) associated with the processes of the addition/dilution. This new model more accurately describes the viability loss seen compared to a simpler maximum volume excursion model which has been described in the past.

### **4.1 Materials and Method**

#### *Oocyte perfusion and image acquisition*

The method for micro-perfusion of oocytes was used to observe osmotic induced volumetric changes of the oocytes during perfusion by using 40X objective magnification and videotaped for image analysis. The videotaped images were digitalized into a series of still images of the oocytes at the given time points.

The calibration factor was determined by the measurement of a cover of a Makler chamber with grids of 0.1 mm by 0.1 mm under the same measurement configuration. The volume and surface area of the oocyte were calculated from this diameter, assuming spherical geometry.

#### *Determination of the permeability coefficients*

A curve-fitting method was used to fit the experimental data and determine the values of  $L_p$  and  $P_s$ . A fixed value for  $V_{bp}$ , determined independently from the Boyle van't Hoff plot, was used in the fitting calculation.

#### *Parthenogenetic activation and development*

At the end of the perfusions, the oocytes were released from the holding pipettes, and collected. These oocytes were then placed into a 1 mol/L sucrose solution to dilute the permeating CPAs from the cytoplasm at room temperature. The durations of the dilutions were 10, 10, and 15 minutes for Me<sub>2</sub>SO, EG, and GLY, respectively. The oocytes were incubated for 30 minutes after two brief washes in mM199, then were parthenogenetically activated by electrical stimulation with three 20  $\mu$ s 3.2 kV cm<sup>-1</sup> DC pulses in activation medium and incubated in mEBSS drops. After 1.5 hours another identical electrical stimulation was applied followed by one hour incubation with 2 mmol/L 6-dimethylaminopurine and 5  $\mu$ g mmol/L<sup>-1</sup> cycloheximide. The oocytes were finally cultured in mEBSS for 4.5 days until the expanded or hatching blastocyst stage, and cleavage, morulae and blastocyst developmental rates were recorded.

#### *Accumulative osmotic damage model*

One model to calculate the accumulative osmotic damage (AOD) caused by volume excursion as was proposed and described by the following equation:

$$\text{AOD} = \int_{start}^{end} \text{abs} \left[ \frac{V_c - V_{iso}}{V_{iso}} \right] \cdot dt, \quad (4.1)$$

## **4.2 Results**

#### *Rabbit oocyte CPA permeabilities*

Membrane permeability data for rabbit oocytes in the presence of different CPAs at room temperature are summarized in Table 4-1.

Table 4-1. Permeability Parameters for Rabbit Oocytes in the presence of Different CPAs (mean  $\pm$  SD)

CPA type	Number of Oocytes	$L_p (\mu\text{m} \cdot \text{min}^{-1} \cdot \text{atm}^{-1})$	$P_s (x 10^{-3} \text{cm} \cdot \text{min}^{-1})$
Me <sub>2</sub> SO	26	0.79 ± 0.26	2.9 ± 1.3
EG	23	0.82 ± 0.22	2.7 ± 1.3
GLY	27	0.64 ± 0.16	0.27 ± 0.18*

\* Indicates a significant difference compared to values within the same column.

### *Blastocyst Development and AOD*

The normalized percentages of blastocyst development after exposure to different CPAs were plotted in relation to the AODs (Table 4-2). These values were strongly correlated ( $r = -0.98$ ; Figure 4.2).

Table 4-2. In Vitro Normalized Blastocyst development of the rabbit oocytes following addition (15% v/v) and dilution of different CPAs in the presence of 1M sucrose and the calculated Accumulative Osmotic Damage (AOD).

	CPA Addition Duration (min)	CPA Dilution Duration (min)	AOD	Normalized Blastocyst Development (%)
Me <sub>2</sub> SO	10	10	407	71
EG	10	10	427	55
GLY	20	15	864	0
Sucrose	6	0	214	84
CONTROL	n/a	n/a	0	100

## 4.3 Discussion

Historically, osmotic damage during CPA addition and removal has been equated solely to the magnitude of the volume changes experienced. As a result, attempts to mitigate this damage have focused on preventing cells from exceeding a specified volume range. On the contrary, the results from the present study suggest that the magnitude of the volume excursion is not the sole predictor of osmotic damage, at least for mammalian oocytes.

Using cell permeability parameters and computer modeling enables simulation of volume changes in various situations of CPA addition and dilution. In the typical volume vs. time plot of cellular volume change, the result of the integration calculation of AOD will be proportional to the area of the curves between the volume line and isotonic volume line. This provides a way to visually estimate the magnitude of AOD. As a first test of the validity of this model, the correlation between the in vitro development potential of the parthenogenetically-activated oocytes and the associate AOD resulting from the CPA addition and dilution procedures have been assessed (Table 4-2). The correlation between these two data sets is strong ( $r = -0.98$ ). In the procedures of CPA addition/dilution, one will always encounter the dilemma of the magnitude versus duration issue: multiple step addition/dilution that decreases the

magnitude prolongs the duration. A more accurate model for describing the effects of both factors should allow the development of improved cryopreservation procedures. The proposed the AOD model is just the first step toward the development of a more comprehensive description of osmotic damage to cells during CPA addition and removal. Future attempts at model development should include the chemical toxicity effect.

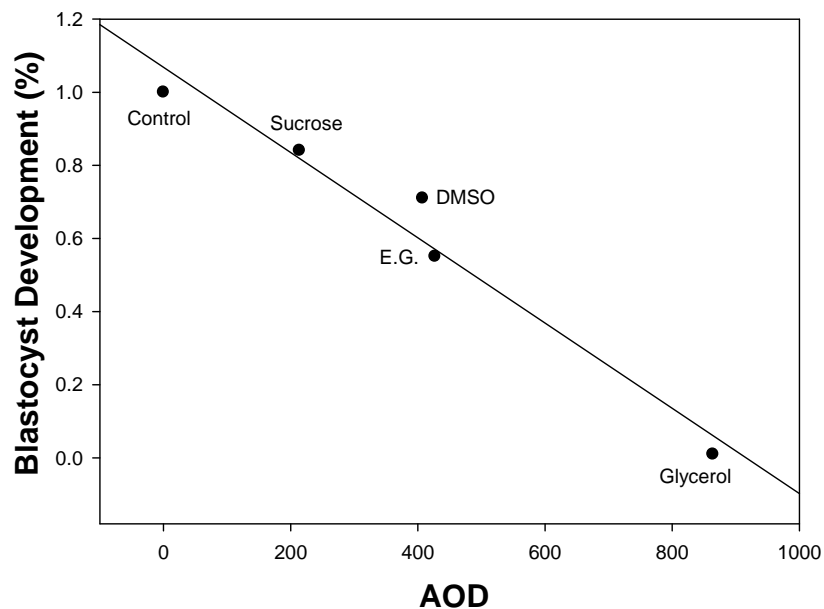


Figure 4.1. Accumulative osmotic damage vs. the normalized blastocyst development percentage of in vitro cultured rabbit oocytes following addition (15% v/v concentration) and dilution of different CPAs in the presence of 1mol/L sucrose. Accumulative Osmotic Damage (AOD) values were calculated by Equation 4. The AOD for the control is zero and normalized development is 1 by definition.

## 5 DEVELOPMENT OF A NOVEL CRYOPRESERVATION THREE-STEP METHOD FOR MAMMALIAN OOCYTE

The difficulties in application of three-step method lie in the determination of the initial CPA concentration, holding temperature,  $T_p$  and holding time,  $t_h$ , for mammalian oocytes. All these conditions are interactive, thus make it impractical to empirically design an optimal protocol. In this thesis, the enhanced and integrated model was developed and applied to a three-step cooling procedure for mouse oocytes. Calculation results are presented in two novel contour plots, from which cryopreservation protocols have been established for mouse oocyte.

### 5.1 Method

*Physical events involved in “three-step” cryopreservation*

First Step: Initially, cells are loaded with CPA at physiologic temperature by introducing them to a solution containing the appropriate concentration and allowing an appropriate equilibration time. Second

\_\_\_\_: When the cell suspension is held at  $T_p$ , the cooling rate becomes zero, so the extracellular CPA concentration remains constant. If the holding time of the second step is sufficiently long, the cell is able to lose enough water via exosmosis to concentrate the intracellular CPA to exceed the  $C_c$ . Third Step: When the intracellular concentration exceeds  $C_c$ , the holding period is terminated by plunging the sample into  $LN_2$ .

#### *Determination of $P_{IIF}$ parameters*

A cryomicroscope system (Hoxan Corporation, Japan) was used to determine the probability of ice nucleation at different temperatures. Mature mouse oocytes were collected from superovulated females using standard procedures. They were placed into a customized glass cell, which was mounted on the cooling chamber of the system with a temperature probe. The chamber was fixed on the stage of an inverted microscope (Nikon, Japan). The incidence of intracellular ice formation can be detected when a sudden refractive index change occurs in the cytoplasm, causing the oocyte to become very dark or opaque when viewed using phase-contrast optics. Temperature dependence of the  $P_{IIF}$  was determined by counting the numbers of cells that had IIF in serial images at different temperatures ( $T$ ), as follows:

$$P_{IIF}(T) = (\text{the number of cells that had IIF at } T) / (\text{the number of total cells})$$

The  $P_{IIF}$  data then were used in a fitting calculation to determine the IIF parameters in Eq 2.5-2.6.

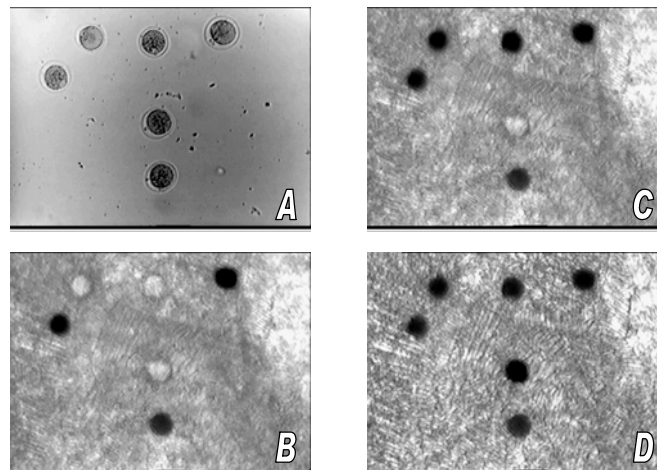


Figure 5.1. Sequence of images captured from a video tape demonstrated the kinetics of IIF for mouse oocytes cooled at  $-40\text{ }^{\circ}\text{C}/\text{min}$  in a 1.5 M DMSO solution. A) before extracellular ice formation at  $-4\text{ }^{\circ}\text{C}$ ; B) Three of six oocytes with intracellular ice formation (IIF) characterized by blackening of the cytoplasm; C) Five of six oocytes with IIF; D) All oocytes have IIF at  $-41\text{ }^{\circ}\text{C}$ .

#### *Presentation of calculation results*

From a practical point of view, the investigation on the  $T_p$  was restricted in the range of  $-20$  to  $-35\text{ }^{\circ}\text{C}$ , and  $C^0$  in the range of 1 M to 4 M. The simulation results can be represented by two contour plots. The first is a contour plot for IIF,  $P_{IIF}$ -Plot. The  $P_{IIF}$ -Plot shows the  $P_{IIF}$  in a percentage scale for each combination of  $T_p$  and  $C^0$  for the corresponding  $t_h$  from  $t_h$ -Plot. It represents the accumulated probability of IIF during the first and the second step. The second contour plot is for the holding time,  $t_h$ -Plot. The  $t_h$ -Plot

shows the time, in seconds, that would be required to hold the cells at the given  $T_p$  and  $C^0$  so that the intracellular CPA concentration would reach the  $C_c$ . If a combination of holding temperature and  $C^0$  will not allow the intracellular solute concentration to reach the  $C_c$ , this combination will have its IIF value assigned to 100%, because intracellular ice formation will occur during plunging into LN<sub>2</sub>.

*Experiments to validate the theoretical predictions.*

To validate the model's prediction of IIF, 4 points on the contour plots that had differing combinations of  $C^0$  and  $T_p$ , and consequently differing values of  $P_{IIF}$  were selected, and 3-step freezing experiments using these conditions were conducted. The factor levels for  $C_0$  were 1.5 and 2.5 M; and for  $T_p$ , -25 and -30 °C. The  $t_h$  was 30 minutes for all treatments. Six replicates were completed. The cells that had lysed during the experiment were scored as having experienced IIF. A 95% confidence interval for the experimental mean percent IIF value was calculated and compared with the theoretically predicted value as a measure of the model's accuracy.

**5.2 Results**

*IIF Observation and Determination of IIF Parameters*

The observation data points of the cryomicroscopy experiment on mouse are plotted in Fig. 5.2 (open circles). The ice formation parameters were determined by fitting the model (Equation 2.5-2.6) to these experimental observations.

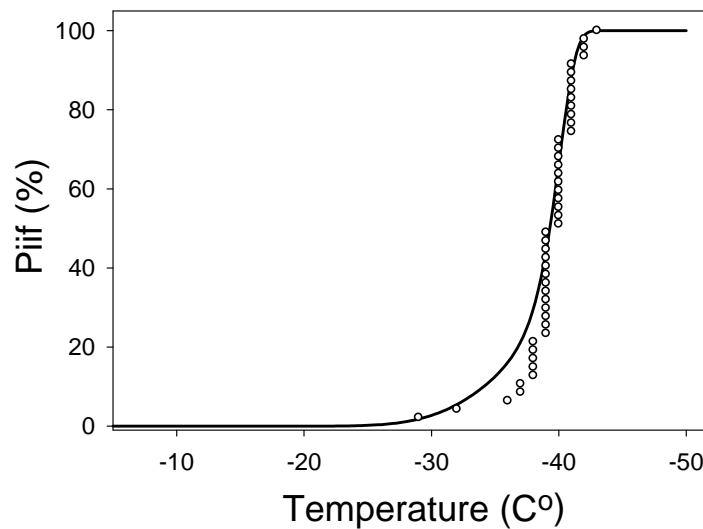


Figure 5.2. Curve fitting to determine the nucleation parameters for mouse oocytes. The experimental observations (open circles) were conducted at cooling rate of 40 °C/min in the presence of 1.5 M DMSO.

*Determination of the  $P_{IIF}$  values for different combinations of  $T_p$ ,  $C^0$ , and  $t_h$*

The calculation results were represented by the  $P_{IIF}$ -Plot showing the  $P_{IIF}$  in a percentage scale and corresponding  $t_h$  for each combination of  $T_p$  and  $C^0$ , over the investigation on the  $T_p$  in the range of -20 to

-35 °C, and  $C^0$  in the range of 1 M to 4 M (Fig. 5.3). It is assumed that 40% was the  $C_c$  of DMSO for mouse oocytes, and 0.29M sucrose was present in this extracellular solution.

#### Optimization of an oocyte freezing protocol

A protocol for three-step mouse oocyte cryopreservation can be readily determined from these contour plots as follows. First, the acceptable  $C^0$  must be determined. It is clear from  $P_{IIF}$ -Plot panel A that there is an inverse relationship between the value of  $C^0$  and the minimum  $P_{IIF}$  attainable. Thus tolerance of the CPA should be known to optimize this procedure. Assuming that an initial DMSO concentration of 2.5M is acceptable, draw a vertical line from the X-axis at this point on panel A up to the point on the contour plot where the  $P_{IIF}$  is acceptable (in this instance we can achieve a predicted  $P_{IIF}$  value of 0). Then the appropriate holding temperature may be determined by referring to the Y-axis at this point, which is -25 °C in this instance. The holding time for this combination can be determined by locating the same point on panel B and identifying the contour line which crosses this point. In this case is it about 1700 seconds. Therefore, the appropriate procedure would be to load the cells with 2.5M DMSO, plunge the straw into a cooling bath set to -25 °C after seeding, hold the straw in this bath for 1700 seconds, and then plunge the straw into liquid nitrogen.

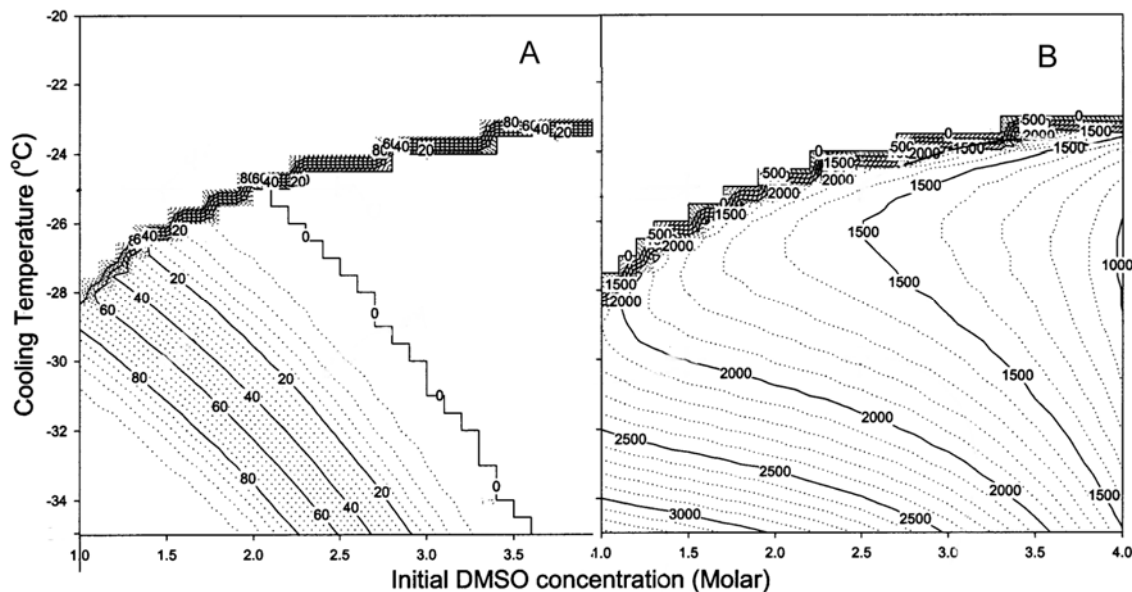


Figure 5.3. Contour graphs of the probability of intracellular ice formation and holding time for mouse MII oocyte. The numbers present the percentage of  $P_{iif}$  in  $P_{iif}$ -Plot and seconds of holding time in  $t_{h}$ -Plot. The critical concentration  $[CPA]_c$  was assumed to be 40% and the extracellular nonpermeating solute osmolality was 600 mOsm.

#### Experimental results versus the theoretical predictions

Figure 5.4 compares the theoretically predicted probability of IIF with the 95% confidence interval for the experimentally-predicted probability for each condition. Three of the four experimental conditions had the theoretically predicted value of  $P_{IIF}$  fall within the confidence interval range.

### 5.3 Discussion

In the area with the absence of contour bars, the values for  $P_{\text{IIF}}$  were assigned to be 100% as stated above. This area encompasses almost all points that have holding temperatures above  $-24\text{ }^{\circ}\text{C}$ . This can be readily explained by examining the phase diagram for a solution of 2.5 M DMSO plus 0.32M NaCl, the solute concentrations will not reach 40% when the temperature is  $-24\text{ }^{\circ}\text{C}$  or above. During the cooling process, the concentration of the extracellular solution will follow the phase diagram, the value being solely determined by temperature for the given solution. The intracellular solute concentration approaches the extracellular concentration during the holding step, but will never exceed it. Therefore, the  $T_p$  must be low enough so that the extracellular solute concentration at the  $T_p$  is great than  $C_c$ .

From the  $P_{\text{IIF}}$ -Plot, the effects of  $C^0$  and  $T_p$  on  $P_{\text{IIF}}$  are explicitly shown. For a given  $T_p$ , the values of  $P_{\text{IIF}}$  decrease as the  $C^0$  increases. Higher intracellular CPA concentrations tend to reduce the extent of supercooling, which is the major factor of  $P_{\text{IIF}}$ . For a given  $C^0$ , the values of  $P_{\text{IIF}}$  increase as the  $T_p$  decreases. Lower holding temperatures increase the extent of supercooling and decrease membrane permeabilities ( $L_p$  and  $P_s$ ) and dehydration. Consequently, this results in a higher  $P_{\text{IIF}}$ .

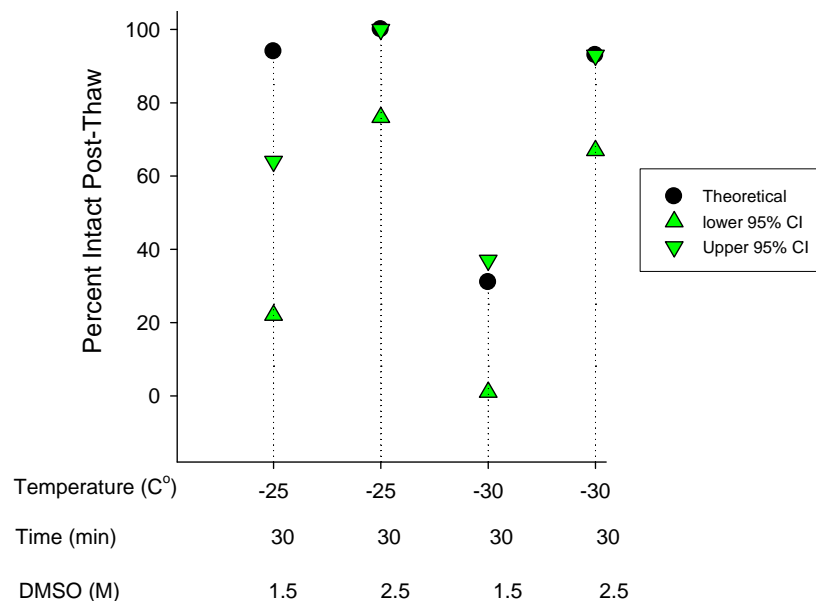


Figure 5.4. Comparison of experimental results to theoretical prediction at various conditions. The experimental survival is estimated as morphology integrity. The theoretical survival is assumed as  $(100 - P_{\text{IIF}})$ .

## 6 NEW SCIENTIFIC RESULTS

1. New coupled equations have been developed to examine the changes of intracellular water volume and the mole number of CPA during temperature changes with cooling rate of  $B$  in the presence of extracellular ice. Two significant improvements have incorporated into this enhanced theoretical

2. The novel methodology has been established to utilize theoretical models for the development of cryopreservation protocols by designing specific cooling profiles and selecting appropriate external conditions to optimize the cryopreservation survivals. The optimum protocol has been determined for rat zygotes.
3. Systematic simulation calculates have been conducted for 2500 cryopreservation conditions and the novel concept of the regions and their cryopreservation relevance have been presented. These regions can be served as the guideline for cryobiologists to design new cryopreservation protocols.
4. The accumulative osmotic damage (AOD) has been proposed for the first time to systematically investigate effects of osmotic stress. The AODs show a very strong correlation to the normalized percentages of blastocyst development after exposure to corresponding CPAs.
5. A novel cryopreservation protocol (three-step) has been designed via a theoretical model that has been enhanced by integrating the ice formation kinetics of three mechanisms of nucleation. For the first time, the ice formation parameters were determined by fitting the model to experimental observations for mouse oocytes. For mouse oocytes, the protocol was established via the theoretical calculation.

## 7 CONCLUSIONS

Cryopreservation methods can be developed by theoretically examining biophysical events during the processes of the cryopreservation. This thesis presents the methodology of utilizing theoretical models for the development of cryopreservation protocols by designing specific cooling profiles and selecting appropriate external conditions to optimize the cryopreservation survivals.

Based on the classic membrane transportation equations (Kedem and Katchalsky formulism) for a ternary solution, a theoretical model that includes the movement of cryoprotectant across the plasma membrane during cooling and warming and the ternary phase diagram was established in the first time. This work had constructed a firm foundation for a comprehensive framework that was established later to optimize one cryopreservation procedure so called the interrupted slow freezing, the prevalent method for oocyte and embryo cryopreservation.

The established model was applied to rat zygotes in the presence of DMSO and contained inside a conventional 0.25 ml cryo-straw. The obtained results for 2500 combinations are plotted on the plane of  $[CPA]_0$  and  $B_1$ , three regions appear with their own characteristics. The concept of the regions and their relevance to cryopreservation was novel. Empirical trial-and-error methodology can hardly achieve this due to limited study points. These regions can be served as the guideline for cryobiologists to design cryopreservation protocol for new cell type. The optimum set of conditions was selected by minimizing duration and determined to be: a  $[CPA]_0$  of 1.2 M DMSO, a  $B_1$  of - 0.95 °C/min and  $T_p$  of -35 °C.

Theoretically, these calculations may be conducted for any cell type and CPA provided the appropriate information regarding the fundamental membrane permeability parameters and phase diagram solution characteristics are known. While the procedures described here focused upon rat zygotes, the cryobiological issues apply directly to other species and other cell types; including mammalian oocytes. However, to use these types of optimization procedures, basic knowledge of the fundamental cryobiology of these cells is required; since different species oocytes and embryos have different cryobiological characteristics.

To systematically investigate effects of osmotic stress, one model was proposed to calculate the accumulative osmotic damage (AOD) caused by volume excursion. Basically, AOD is an integration of the relative volume excursion of the oocyte over the whole duration of the procedure. The AOD values were used to assess the correlation between the in vitro development potential of the parthenogenetically activated oocytes. It could be concluded that the osmotic damage associated with CPA addition and removal is accurately described by both a magnitude and duration using an accumulated osmotic damage model.

In the procedures of CPA addition/dilution, one will always encounter the dilemma of the magnitude versus duration issue: multiple step addition/dilution that decreases the magnitude prolongs the duration. Historically, osmotic damage during CPA addition and removal has been focused on the magnitude of the volume changes experienced. As a result, attempts to mitigate this damage have focused on preventing cells from exceeding a specified volume range. The current more accurate AOD model for describing the effects of both factors should allow the development of improved cryopreservation procedures. Recently, CPA dilution condition in the procedure of oocyte cryopreservation has been given more attention. The current AOD model should be a useful tool to examine these approaches, or even optimize these approaches. This AOD model is a first step toward the development of a more comprehensive description of osmotic damage to cells during CPA addition and removal. Future attempts at model development should include the inclusion of a chemical toxicity effect. Also future studies should independently test this model to determine if it is more broadly applicable.

In this thesis, the theoretical model introduced in the previous chapter was enhanced by integrating the ice formation kinetics that includes three mechanisms. For mouse oocytes, the novel protocol was established via the theoretical calculation as the following: to load the cells with 2.5M DMSO, plunge the straw into a cooling bath set to  $-25^{\circ}\text{C}$  after seeding, hold the straw in this bath for 1700 seconds, and then plunge the straw into liquid nitrogen.

The constructed model can estimate the  $P_{\text{IF}}$  under different experimental conditions, and these values can be compared with experimental results. Seventy five percent of experimental conditions had the theoretically predicted value of  $P_{\text{IF}}$  fall within the confidence interval range.

The present study outlines a process whereby fundamental principles of cryobiology have been applied to the design of a cryopreservation procedure intended to overcome challenges unique to

mammalian oocyte. By integrating theoretical concepts and experimental observations, this model was developed to predict the likelihood of intracellular ice formation for combinations of DMSO concentrations, holding times, and holding temperatures in a 3-step freezing design. It remains to be seen if this approach will also preserve the developmental potential of the oocytes.

## 8 PUBLICATIONS RELATED TO MAMMANLIAN OOCYTE CRYOPRESERVATION

1. Agca, Y., **Liu, J.**, Critser, E. S., and Critser, J. K. (2000a). Fundamental cryobiology of rat immature and mature oocytes: hydraulic conductivity in the presence of Me(2)SO, Me(2)SO permeability, and their activation energies. *J Exp Zool* **286**, 523-33.
2. Agca, Y., **Liu, J.**, Critser, E. S., McGrath, J. J., and Critser, J. K. (1999). Temperature-dependent osmotic behavior of germinal vesicle and metaphase II stage bovine oocytes in the presence of Me2SO in relationship to cryobiology. *Mol Reprod Dev* **53**, 59-67.
3. Agca, Y., **Liu, J.**, McGrath, J. J., Peter, A. T., Critser, E. S., and Critser, J. K. (1998a). Membrane permeability characteristics of metaphase II mouse oocytes at various temperatures in the presence of Me2SO. *Cryobiology* **36**, 287-300.
4. Agca, Y., **Liu, J.**, Peter, A. T., Critser, E. S., and Critser, J. K. (1998b). Effect of developmental stage on bovine oocyte plasma membrane water and cryoprotectant permeability characteristics. *Mol Reprod Dev* **49**, 408-15.
5. Agca, Y., **Liu, J.**, Rutledge, J. J., Critser, E. S., and Critser, J. K. (2000b). Effect of osmotic stress on the developmental competence of germinal vesicle and metaphase II stage bovine cumulus oocyte complexes and its relevance to cryopreservation. *Mol Reprod Dev* **55**, 212-9.
6. Dinnyes, A., **Liu, J.**, and Nedambale, T. L. (2007). Novel gamete storage. *Reprod Fertil Dev* **19**, 719-31.
7. **Liu, J.**, Mullen, S., Meng, Q., Critser, J., and Dinnyes, A. (2009). Determination of oocyte membrane permeability coefficients and their application to cryopreservation in a rabbit model. *Cryobiology* **59**, 127-34.
8. **Liu, J.**, Woods, E. J., Agca, Y., Critser, E. S., and Critser, J. K. (2000). Cryobiology of rat embryos II: A theoretical model for the development of interrupted slow freezing procedures. *Biol Reprod* **63**, 1303-12.
9. **Liu, J.**, Zieger, M. A., Lakey, J. R., Woods, E. J., and Critser, J. K. (1997). The determination of membrane permeability coefficients of canine pancreatic islet cells and their application to islet cryopreservation. *Cryobiology* **35**, 1-13.
10. Pfaff, R. T., Agca, Y., **Liu, J.**, Woods, E. J., Peter, A. T., and Critser, J. K. (2000). Cryobiology of rat embryos I: determination of zygote membrane permeability coefficients for water and cryoprotectants, their activation energies, and the development of improved cryopreservation methods. *Biol Reprod* **63**, 1294-302.
11. Pfaff, R. T., **Liu, J.**, Gao, D., Peter, A. T., Li, T. K., and Critser, J. K. (1998). Water and DMSO membrane permeability characteristics of in-vivo- and in-vitro-derived and cultured murine oocytes and embryos. *Mol Hum Reprod* **4**, 51-9.
12. Van den Abbeel, E., Schneider, U., **Liu, J.**, Agca, Y., Critser, J. K., and Van Steirteghem, A. (2007). Osmotic responses and tolerance limits to changes in external osmolalities, and oolemma permeability characteristics, of human in vitro matured MII oocytes. *Hum Reprod* **22**, 1959-72.